

	nBLM Project – CDR1.1	CEA-ESS-DIA-RP-0033
	ESS-I	

REPORT

NBLM PROJECT CDR11

	REDACTEUR <i>Edited by</i>	VERIFICATEURS <i>Reviewed by</i>		APPROBATEUR <i>Approved by</i>
NOM Prénom <i>Name</i>	SEGUI Laura	PAPAEVANGELOU Thomas		PAPAEVANGELOU Thomas
Fonctions <i>Functions</i>		PI		PI
Date et signatures <i>Date and visas</i>				



 	nBLM Project – CDR1.1	CEA-ESS-DIA-RP-0033
	ESS-I	Page 2 sur 43

CARTOUCHE D'EVOLUTION - DOCUMENT REVISION HISTORY			
Éditions <i>Editions</i>	Dates <i>Dates</i>	§ modifiés <i>Modified part(s)</i>	Commentaires – <i>Observations</i>
A		Tous	Création



LISTE DE DIFFUSION – DISTRIBUTION LIST	
<u>Interne - Internal :</u> - nBLM team	<u>Externe - External :</u> - ESS
Copies – Copy to :	

CONTENTS

1. Introduction	5
1.1. Purpose	5
1.2. List of acronyms and abbreviations	5
1.3. Documents sent in nBLM CDR1.1 package	6
2. Description of detector objective	6
3. Prototype Tests and design modification	8
3.1. Results	8
3.1.1. Electronic studies	8
3.1.2. Gain stability and gas studies	10
3.1.3. Detector response studies	11
3.1.4. Tests at Birmingham irradiation facility	12
3.2. New detector design	12
3.2.1. Gas chamber	13
3.2.2. Slow Detector	14
3.2.3. Fast Detector	16
3.2.4. Micromegas Detector	16
3.3. Gas system recirculation	17
3.4. Tests planned for 2018	19
4. Electronics overview	22
4.1. Electronics components	22
4.2. Hardware for High Voltage and Low voltage	23
4.2.1. Crate CAEN SY4527	23
4.2.2. High Voltages	24
4.2.3. Low voltage	25
5. Front-End Electronics	26
5.1. PCB designs	26
5.1.1. Signal read mezzanine card	26
5.1.2. HV mezzanine card	28
5.2. Cables and patch panels connectors	29
6. BEE and Acquisition	30
6.1. MTCA crate	30
6.2. Fast acquisition	30
6.3. FPGA software	31
7. nBLM Control system	32
8. Gas system status	32
9. nBLM systems risk analysis	33
10. nBLM system architecture at ESS	34
10.1. Distribution of nBLM detectors along the accelerator	34
10.2. Detector acquisitions and racks distribution	36

 	nBLM Project – CDR1.1	CEA-ESS-DIA-RP-0033
	ESS-I	Page 4 sur 43

10.3.	Power supplies distribution	37
10.4.	Gas lines distribution in the accelerator	37
10.5.	Position and preliminary design of patch panels in accelerator tunnel	40
10.5.1.	Gas in accelerator tunnel.....	40
10.5.2.	Electronics patch panel in accelerator tunnel	41
10.6.	Preliminary design of detectors support structure	41
10.7.	Procurement of components.....	42

 	nBLM Project – CDR1.1	CEA-ESS-DIA-RP-0033
	ESS-I	Page 5 sur 43

1. Introduction

1.1. Purpose

This is the first of the 2 CDRs foreseen for the nBLM system and, according to the technical annex, it is focused on the electronics design. Initial results from the prototype detector and electronics test are also covered in the review. In order to meet the installation schedule some activities have been pulled forward. These involve long-haul cabling and tunnel gas piping; therefore, layout of these components are included in the review. Detail verification plan and potential safety hazards are not within the scope of this review, but will be covered in the final CDR, as well as for the final gas system design.

The document is complemented with further documentation listed in section 1.3.

1.2. List of acronyms and abbreviations

Name or acronym	Definition
BEE	Back-End Electronics
BIS	Beam Interlock System
BNC	Bayonet Neill–Concelman (Connector)
CA	Channel Access
CEA	Commissariat à l'Energie Atomique
CPU	Central Processor Unit
CS	Control System
DTL	Drift Tube Linac
EEE	ESS EPICS Environment
ESS	European Spallation Source ERIC
EPICS	Experimental Physics and Industrial Control System
ESSI	ESS Irfu project
FEE	Front-End Electronics
FPGA	Field Programmable Gate Array
GND	Ground
GUI	Graphical User Interface
HEBT	High Energy Beam Transport
HWR	Half Wave Resonator
IKA	In-kind agreement
I/O	Input / Output
ICS	Integrated Control System
LCS	Local Control System
LINAC	Linear Accelerator
MCA	Multi-channel Analyzer
MEBT	Medium Energy Beam Transport
MMs	Micromegas detector
MPGD	Multi Pattern Gaseous Detectors
MPS	Machine Protection System
MTCA	Micro Telecommunications Computing Architecture

nBLM	Neutron sensitive Beam Lost Monitor
PA	Preamplifier
PCB	Printed Circuit Board
PDR	Preliminary Design Review
PLC	Programmable Logic Controller
PV	Process Variable
P&ID	Piping and Instrumentation Diagram
SAR	System Acceptance Review
SMA	SubMiniature version A (Connector)
SoW	Scope of Work
SHV	Safe High Voltage (Connector)
TBC	To Be Confirmed
ToT	Time Over Threshold

1.3. Documents sent in nBLM CDR1.1 package

Ref.	Document
	Capteur lent zone centrale V4-1 Dossier de plans rév B.pdf
	Zone capteur étanche rapide V4-1 - dossier de plans Rev B.pdf
	nBLM_CDR11_SlowvsFast_nBLM_Detector.pdf
	nBLM_subsystemsRiskAnalysis.pdf
	nBLM control system design.pdf

2. Description of detector objective

In the review of the PDR1.2 [1], documentation of the mode and detector that cover every lost was requested. Moreover, a clear description of the functionalities and expected responses of them was also requested. In the document “*nBLM_CDR11_SlowvsFast_nBLM_Detector.pdf*” attached to the CDR1.1 package we try to answer to these requirements. In this section we just give an overview.

The nBLM system is a new Beam Loss Monitor based on the detection of neutrons using a Micromegas detector. It is complementary to other BLM systems in ESS. It was originally conceived to operate in counting mode, in the region where others BLMs have a small sensibility, i.e. in the low energy region of the accelerator. The expected rate during normal operation discussed during the conceptual design of the system was of few n/s. In addition, in the low energy region, only neutral particles (neutrons and photons) are able to escape from the accelerator. The detector we propose is only sensitive to neutrons and insensitive to gammas, presenting a big advantage compared with icBLM where an x-ray background from the RF could hide or mimic a lost from the accelerator.


Micromegas [2] detectors are a type of MPGD (MultiPattern Gaseous Detectors) used very extensively in a wide range of particle physics experiments, including neutron detection, for example in the nTOF experiment. As indicated by its name it is a gaseous detector where the charged particles arriving to the chamber will ionize the gas and this ionization is amplified and detected in the Micromegas detector.

The expected signal in a Micromegas detector are of few mV. The requirements from ESS for such a system is to be able to give a response in 5 μ s and to be able to monitor losses of 100 mW/m.

The detectors we propose are in fact the combination of two detectors, that we call “Slow” and “Fast”, based on their time response. However, they have also another differences between them, mainly determined by the way the neutrons are converted into charged particles that produce a signal in the chamber. A Micromegas detector, as any ionization detector, detects charged particles, therefore, we need to use a convertor in order to detect the neutrons. In the aforementioned document a comparison between the signal formation, the expected sensitivity and the expected function of each one is discussed. They were conceived to have a complementary functionality. In Table 1 the characteristics of each detector are summarized.

	SLOW	FAST
Convertor	B ₄ C	Mylar or Polypropylene
Reaction	(n, α) ¹⁰ B	(n,p)
Signal	Fast neutrons after moderation	Fast neutrons
Detected energy	~constant	Continuum distribution of energies
Sensitivity	10 ⁻⁶ < En < 100 MeV	En > 0.5 MeV
Solid angle	4 π	2 π , n coming from the front only
Efficiency	~few n·cm ⁻² ·s ⁻¹	~10-100 times smaller
Response time	~200 μ s	~0.01 μ s
Objective	Monitoring of small losses	Alarm (in 5 μ s) Fine structure of the lost
Shielding	Yes, for thermal neutrons	Not needed

Table 1: Summary of the characteristics of each detector. Note that “En” is the energy of the neutron detected.

	nBLM Project – CDR1.1	CEA-ESS-DIA-RP-0033
	ESS-I	Page 8 sur 43

3. Prototype Tests and design modification

The first prototypes discussed in [3] and [4] have been tested in the DEDIP laboratory. Other tests are foreseen in different irradiation facilities discussed in section 3.4.

In the following we present the tests done so far with the detectors and the modifications that we introduce in the design of the detectors after those initial tests. Some of the tests were already discussed in [4].

3.1. Results

3.1.1. Electronic studies

Several results were already shown in [4]. The performed tests are summarized in the following list:


- Study of the gain of the preamplifiers
- Study of the effect of long cable (placed after the amplifiers) in:
 - Rise Time
 - Pulse Duration
 - Pulse amplitude
- Study of the effect of long cable (placed *BEFORE* the amplifiers)

Effect of long cable in signal delayed

A delay of ~150ns was measured after a 50m cable used for the transmission of the signal compared with 1m cable. Assuming a linear relation and taking into account that the maximum expected length of cable is of 80m, a delay of maximum 240ns will be introduced to the signal. The contribution to the whole time budget is of 5%.

Effect of long cable in signal shape

Negligible effect on amplitude was observed. For the rise time, with a cable of 40m, for an initial signal of 5 ns rise time, the measured rise time is ~17ns, while for an initial signal of 35 ns rise time, the output after 40 m is ~40ns. As the expected signal has a rise time of ~30-50 ns the effect of a long cable does not have an effect. The duration of the pulse is driven by the drift distance, therefore the length of the cable has no effect on the pulse duration.

	nBLM Project – CDR1.1	CEA-ESS-DIA-RP-0033
	ESS-I	Page 9 sur 43

Placement of amplifiers after long cable

Another suggestion from the PDR1.2 reviewers was to study the effect of placing the electronics far away from the detector and not on-board as proposed. Note that the expected signal in a Micromegas detector is of few mV and few μ A. In any case, studies have been performed. However, we were reading the mesh and not the anode as the actual preamplifiers are already on-board and we can't put any cable before them. In addition we were using charge preamplifiers not the fast we are going to use.

When reading the mesh we were using a charge preamplifier ORTEC 142B. A cable of ~ 0.5 m and another of 50m were connected from the mesh to the PA, i.e. the long cables is placed before the FEE. The signals were then send to a shaper amplifier. Results are shown in Figure 1 showing the spectra recorded with a Multi-Channel Analyser (MCA). Both spectra were recorded in the same time. There is a clear increase in the noise and a decrease in the rate in the peak. Even if it is not using the same preamplifiers, this test allows to conclude the effect of using the long cable before the preamplifier.

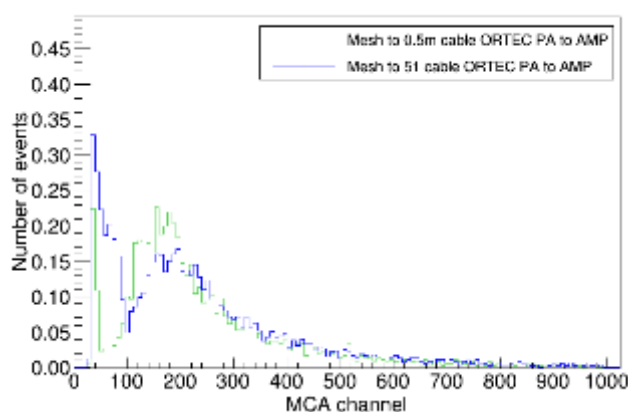


Figure 1: Comparison of the energy spectrum measured from the slow nBLM detector using a MCA with a long and a short cable placed before the charge preamplifier.

FMC-3111 and IFC-1410 test

A local installation of the EPICs environment into the IFC-1410 has been done the 03/11/2017 by ESS-ICS. The full acquisition chain has been tested with one of the nBLM detectors the 17/11/2017 showing good performance in this initial test. However more studies are needed in order to verify the capabilities required from this system: high rates and no dead time.

3.1.2. Gain stability and gas studies

Studies have been carried out regarding the gain stability of the detector. First with the gas circulating in open mode and then closing the detector and stopping the gas flux. The mentioned study was also requested by the reviewers of document PDR1.2 [4]. A test circulating the gas in closed mode through a filter has been also performed and is discussed in subsection 3.3.

Data has been recorded reading the mesh of the nBLM slow detector. We use the slow module as we know the deposited energy distribution has a peak as the detected signal has always the same energy. The peak position is monitored to study the gain stability. The electronics chain used was an ORTEC 142-B PA connected to a spectroscopy amplifier ORTEC 672 and we send the pulses to an AMPTEK MCA-8000. A spectrum is recorded every 20minutes and is fitted offline. The evolution of the peak is then plotted to study the gain stability. In addition the rate is also calculated as the area under the peak. A typical spectrum with the fit is shown in Figure 2. The defined function for the fit is a convolution of a Landau (ideal spectrum) plus an exponential and a flat background. Although if the fit has a bad χ^2 it is good enough to find the position of the peak to study the gain stability.

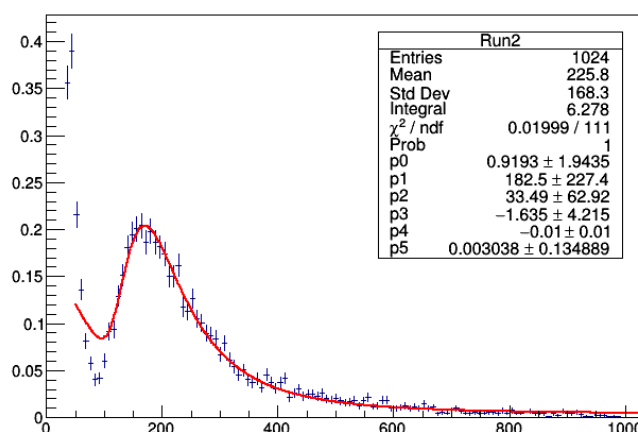


Figure 2: Example of spectrum reconstructed in the MCA from the slow detector reading the mesh with a charge PA+ amplifier. The source used is Cf-252. The spectrum is fit and the position of the peak is saved in order to study the evolution of the gain with respect time.

In Figure 3 (a) the evolution of the gain for 24h with gas circulating in open mode is shown. We can see how the detector is stable within a 10% variation. The slope of the best fit is compatible with zero. In Figure 3 (b) the evolution of the peak with the detector in sealed mode is shown, i.e. with the chamber filled of gas but closed. After 5h the gain drops a 30%, after 12h a 50% and after one day there is no signal over background but the detector does not show discharges. However, it is interesting to notice, that, when the detector is reopen an under pressure is observed. That means that the leak is Helium escaping and not air entering the system. Helium is one of the lightest gases

and can easily enter or escape from volumes. On the other hand it has been chosen due to its good discrimination capabilities between neutron and gammas.

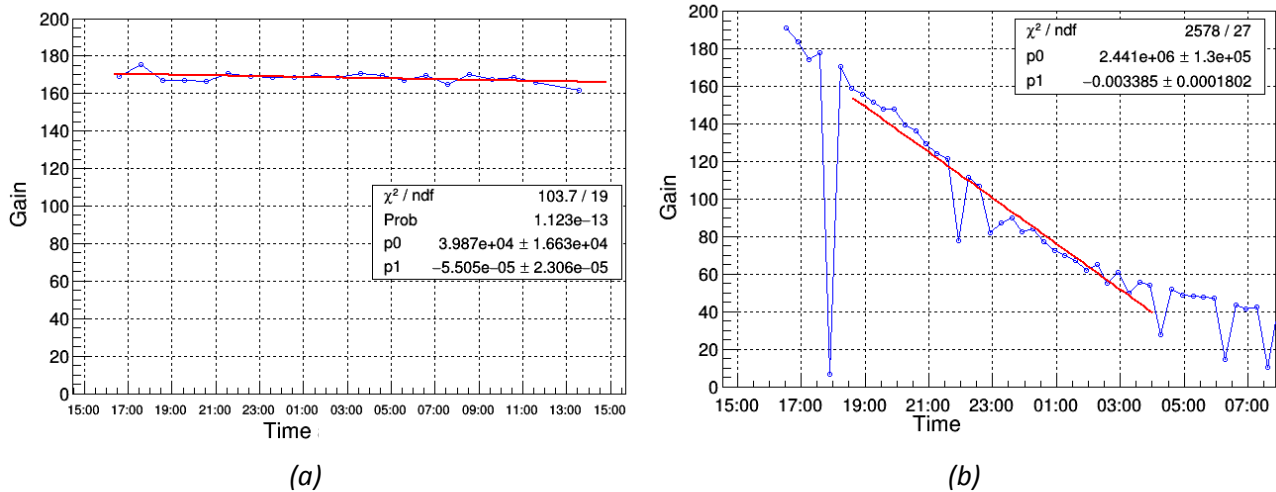


Figure 3: Position of the peak mesh spectrum with respect time. (a) Gas circulation in open mode. (b) Gas circulation closed.

3.1.3. Detector response studies

Both detectors, fast and slow have been tested with a Cf-252 source in the DEDIP laboratory with very low rates. The mounted detectors are shown in Figure 4. The data taken has been recorded using an oscilloscope directly after the preamplifiers. This initial campaign has allowed to develop analysis algorithms to help defining the algorithm for the FPGA that is on-going. Moreover, we have seen signals in both detectors and we have been also able to study the amplifier gain and the signal to noise ratio. For the slow we have tested two different B4C thicknesses and two different drift distances. For the slow we have used a 100 μm aluminized mylar foil. However the measurements for the characterization and optimization of the detectors need much higher neutron and gamma fluxes and would be done according to the planning shown in section 3.3.

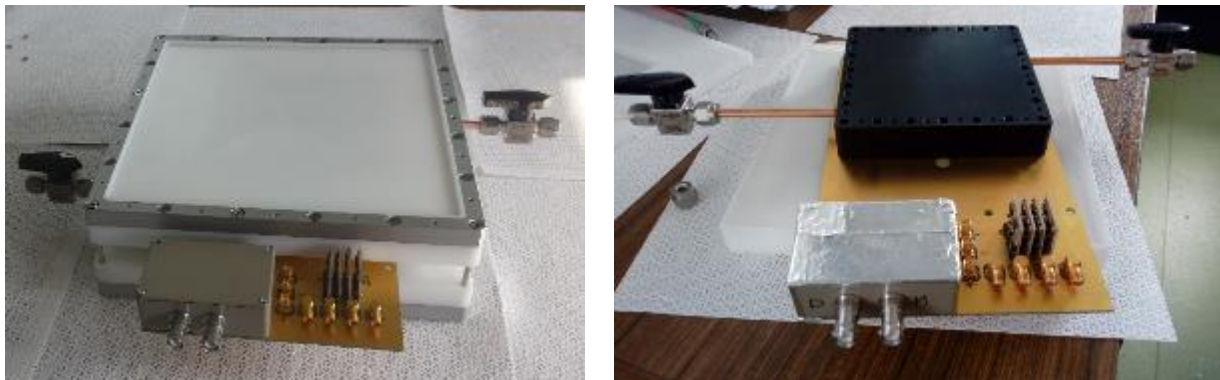



Figure 4: Slow and fast detector mounted for tests at DEDIP.

	nBLM Project – CDR1.1	CEA-ESS-DIA-RP-0033
	ESS-I	Page 12 sur 43

3.1.4. Tests at Birmingham irradiation facility

In section 3.7 a full list of the planned tests to be carried out during the first semester of 2018 is shown. The first test is happening few days before the presentation of the CDR1.1 (from the 26th to 29th of November) to perform studies with the nBLM slow detector. The aim of the test is to record signals produced when a proton beam irradiates a material producing a cascade of secondary particles. In addition, electronics components can be irradiated to a fluence of 10^{15} 1MeV n_{eq} cm⁻² in 80s at 1μA and we can leave some samples at Birmingham for the required time to reach the expected level at ESS.

We expect to present some feedback of the tests during the CDR1.1 presentations.


3.2. New detector design

After the studies performed with the initial prototypes, a new design of the detectors, both for the mechanics and for the electronics, has been done and it is proposed in this document. The electronics have been changed to have the amplifiers and the HV and LV connectors in mezzanine cards. The choice of the mezzanine cards gives flexibility for the replacement of FEE if needed and even flexibility in the design if special purpose detector is requested. In addition we reduce the manipulation on the detector card after the bulking process. In this section the mechanical design is explained in detail. The electronics designed is covered in section 4.

The main change is an improvement in the electronics shielding: the PCB board of the detector and the mezzanine cards will be enclosed in an aluminium box of 1.5 mm thickness. One of the side of this box will be a patch panel with the connectors to the cables and the gas as it can be seen in Figure 5. In addition, with this new design we make easier the installation, the connections and the grounding as well as the protection of the detector.

The design of both detectors together is shown in Figure 5 and in Figure 6. Both detectors can be used assembly or separately, as in the case of the prototypes.

The new design has been carried out having in mind the final design. We expect only minimal things to be changed. As for the previous prototypes, they have been conceived to be flexible in the polyethylene thickness, drift distance and convertors thickness. These are the main changes we expect between this proposed design and the final one, where the parameters will be fixed. However, for the final design, we will also want to be flexible with some of these values, to adapt to the real rates during commissioning. In that sense, we want to have the possibility to use different convertors

	nBLM Project – CDR1.1	CEA-ESS-DIA-RP-0033
	ESS-I	Page 13 sur 43

thicknesses without changing the mechanics to be adaptable to different radiation fluxes or to change the polyethylene thicknesses.

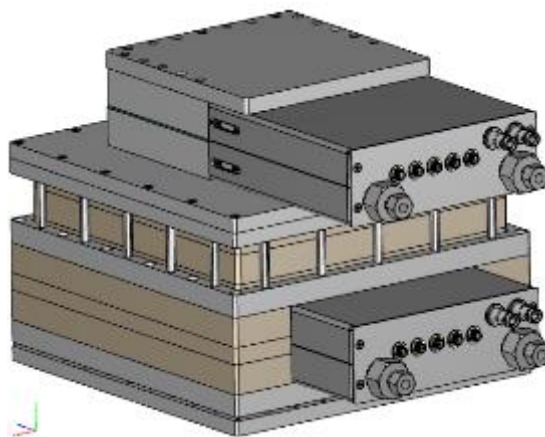


Figure 5: New nBLM detectors design. The “fast” module is seen in the top side of the detector, while the “slow” module is attached below it. As in the previous design both detectors can be used assembly together or separated.

3.2.1. Gas chamber

The gas chamber is designed identical for both detectors, fast and slow. A figure is shown in Figure 6. The chamber is closed using o-rings made by rubber, same material as used at CERN. The gas tubes are designed in copper that is tighten and glued in the aluminium box of 1.5 mm thickness in top and bottom and 12 mm in laterals. We are investigating alternatives for the glue or to identify a one that can be radiation resistant. Also, the possibility to use plastic tubes is also under investigation. In addition, the use a radiation resistance rubber is also under investigation.

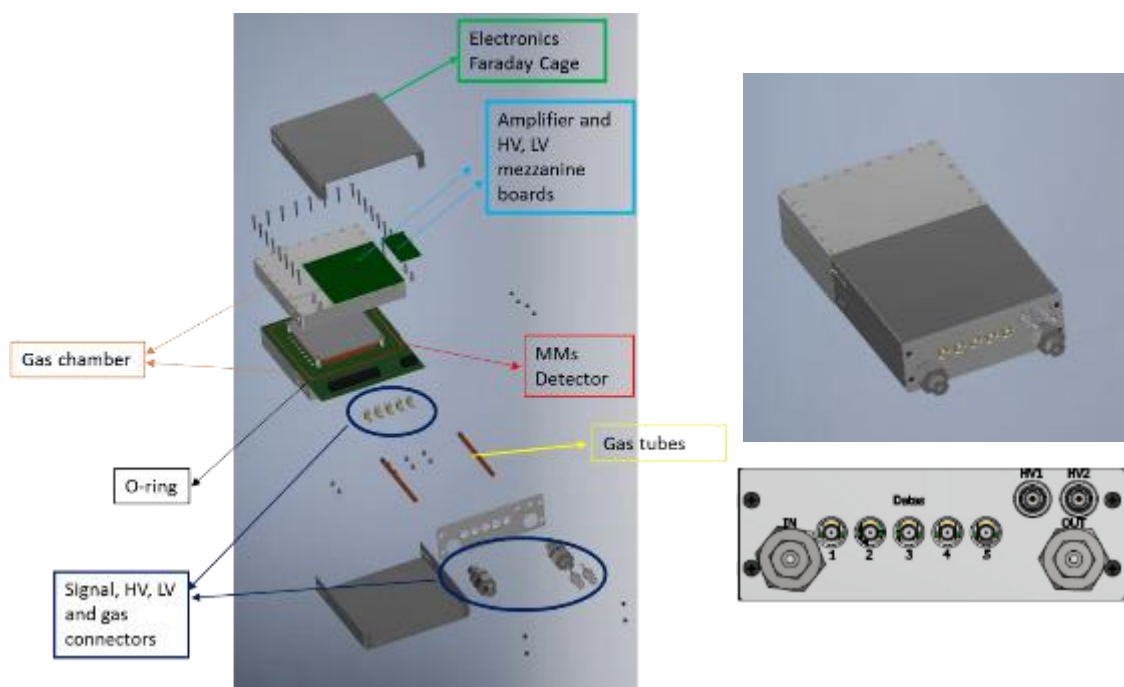


Figure 6: nBLM gas chamber: (Left) open detailing each element. (Right-top) Closed (Right-bottom) Detailed of patch panel in box.

3.2.2. Slow Detector

The main difference between the detectors is that the slow chamber is surrounded by polyethylene. As mentioned previously, it has the versatility to install different polyethylene thicknesses. In addition, an external layer of borated rubber (few mm) can be placed between the metallic frame and the last polyethylene layer, in order to reduce further the thermal neutrons contribution. The design with respect to the prototypes presented in [3] has not changed. A 3D view is shown in *Figure 7 a)* and *b)*. The general 2D plan is shown in *Figure 8* while all the plans and details are sent attached with this document.

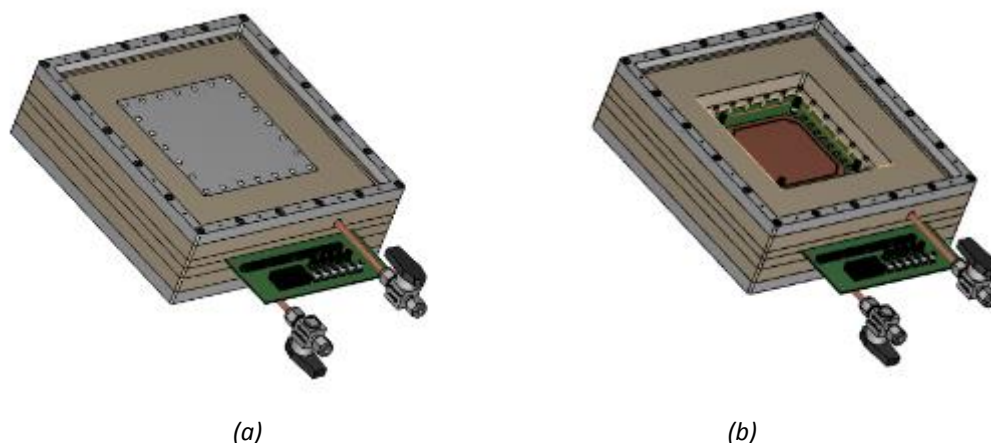


Figure 7: 3D view of the slow detector closed (a) and open (b).

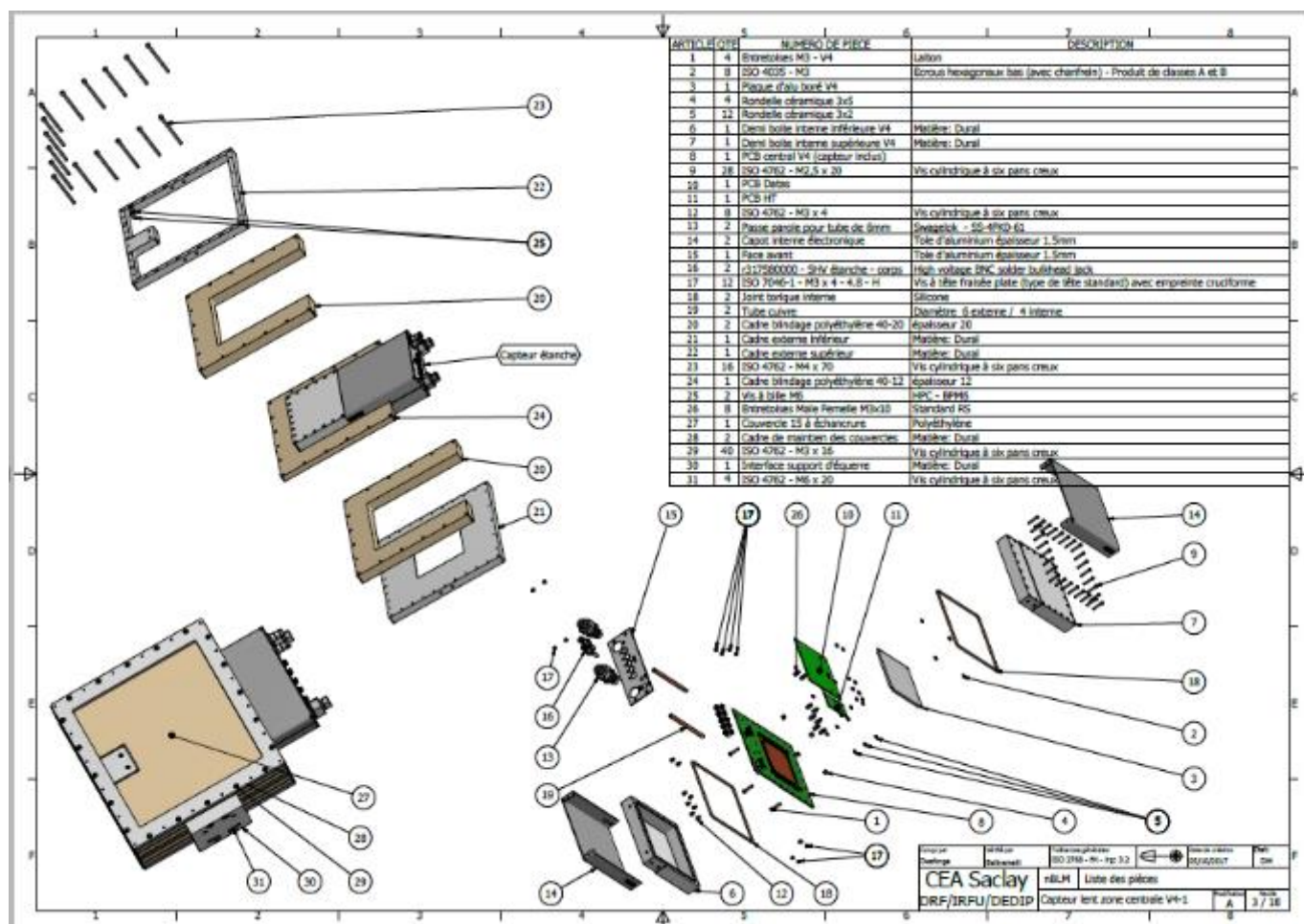
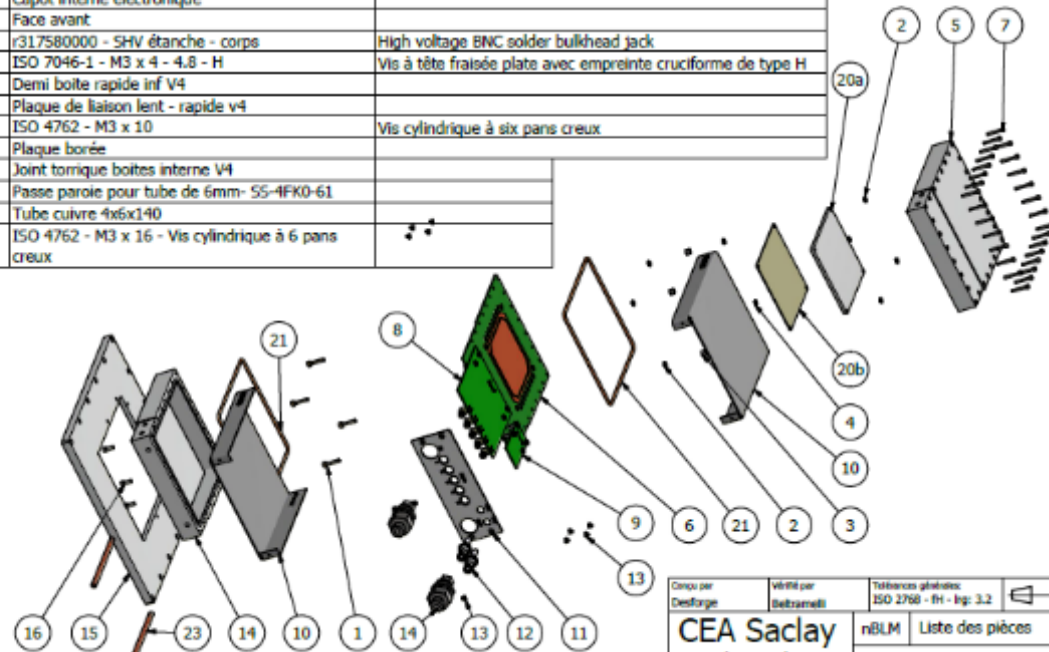


Figure 8: Expanded view of the "slow" detector.

3.2.3. Fast Detector

The addition of the electronics shielding is the only change for the fast detector with respect to the prototypes designed shown in [3]. The expanded view is shown in Figure 9.

LISTE DE PIÈCES				Note: La plupart des pièces sont communes avec le capteur lent. les principales différences se portent sur la pièce [14] ainsi que sur les pièces spécifiques [15] et [20].
ARTICLE	QTE	NUMERO DE PIECE	DESCRIPTION	
1	4	Entretroises M3 - V4		Les PCB et leurs composants font l'objet d'un second dossier de plans
2	8	ISO 4035 - M3	Ecrous hexagonaux bas (avec chanfrein)	
3	4	Rondelle céramique 3x5		Les pièces [17] à [19] concernant le blindage plomb ne sont plus utilisées (Modification A)
4	4	Rondelle céramique 3x2		
5	1	Demi boîte interne supérieure Rapide V4-1		
6	1	Assemblage PCB central		
7	28	ISO 4762 - M2,5 x 20	Vis cylindrique à six pans creux	
8	1	PCB Datas		
9	1	PCB HT		
10	2	Capot interne électronique		
11	1	Face avant		
12	2	r317580000 - SHV étanche - corps	High voltage BNC solder bulkhead jack	
13	12	ISO 7046-1 - M3 x 4 - 4.8 - H	Vis à tête fraisée plate avec empreinte cruciforme de type H	
14	1	Demi boîte rapide inf V4		
15	1	Plaque de liaison lent - rapide v4		
16	15	ISO 4762 - M3 x 10	Vis cylindrique à six pans creux	
20	1	Plaque borée		
21	2	Joint torique boîtes internes V4		
22	2	Passerelle pour tube de 6mm- SS-4FK0-61		
23	2	Tube cuivre 4x6x140		
24	20	ISO 4762 - M3 x 16 - Vis cylindrique à 6 pans creux		



Conçu par Desfray	Vérifié par Beltzmann	Tolérances géométriques ISO 2768 - H - fig: 3.2	Date de création 05/10/2017	État A
CEA Saclay DRF/IRFU/SEDI		nBLM Liste des pièces 66-Q051-DM-0200-Capteur rapide		
		Modification A	Feuille 2 / 11	

Figure 9: Expanded view of the “fast” detector.

3.2.4. Micromegas Detector

Regarding the detector itself, nothing has been changed for the new design concerning the sensitive area. However, as we will give the power and read the signal through the independent mezzanine cards explained in Section 4, the PCB board has been adapted to integrate the appropriate connectors.

We will manufacture 3x3 detectors per PCB as shown in Figure 10. We have ordered 2 boards initially and we expect to launch the production of 10-12 boards by June 2018. The PCBs will be manufactured

in an external company, ELVIA, with who DEDIP collaborates habitually. The bulking of the detectors will be performed at the MPGD workshop in the CEA/Saclay DEDIP laboratory. One board can be bulk per day. Including the preparation of the machines and the bulk of the 12 boards, all the detectors can be ready in 15-20 working days (1 month).

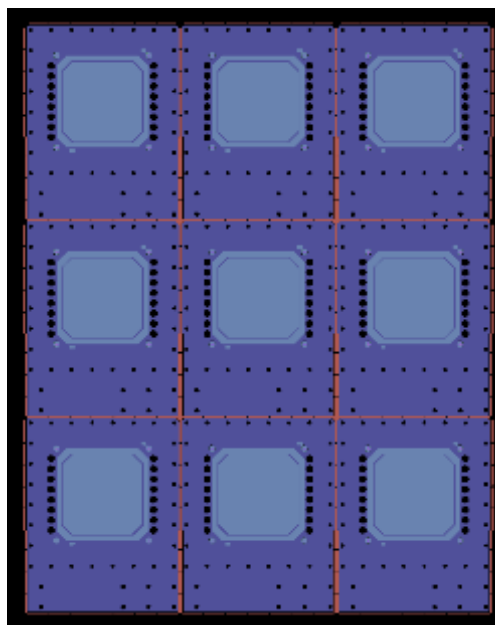


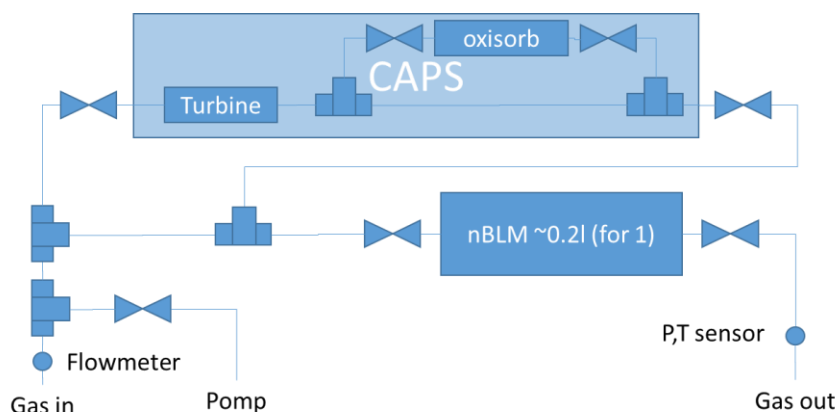
Figure 10: PCB board design to house 9 MMs PCB boards

3.3. Gas system recirculation

The detector ($V_{det} \sim 0.2l$) is designed to operate at open gas circulation mode. However, for some of the foreseen tests we will have to operate in sealed mode due to the restrictions in accessibility once installed and the no possibility to install in the installations we are going a gas system. The main test with these constraints is the test at LINAC4. Therefore, we decide to use a gas system recirculation developed from HARPO experiment¹. The idea is to keep a good specification of the detector during all the time of it the test. The principle is to use a turbine and O₂/ H₂O filters. This principle is explain in a patent². Also it has to be compact.

¹ <https://arxiv.org/abs/1706.06483>

² <https://arxiv.org/abs/1512.03248> <http://bases-brevets.inpi.fr/fr/document/EP3054168.html>



Several modes are possible. The first one is to clean the system and the detector by flushing it (principle of degassing). So most of the valves are open and the gas is circulated at $\sim 5\text{l/h}$ during 1-2 hour(s). The second mode corresponds to the use of the detector as usual to determine its point of operation (mesh / drift voltages to have the best gain / dynamic / sensibility). A third mode lets the possibility to close all the gas CAPS and let the detector work. At this mode we can observe that the gain is decreasing in several hours, so the gas in the system doesn't let to reach the specifications. The last mode is to recirculate the gas by using the "turbine" and passing the gas through the filter to keep the purity of the gas stable and therefore the gain.

The circulator is composed of a simple turbine shown in Figure 11. The gas is pass through an Oxisorb purification cartridge that can absorb up to $0.5\text{l H}_2\text{O}$ and 0.1l O_2 , with output purity as low as $< 5\text{ ppb}$ for O_2 and 30 ppb for H_2O .

As it's not a product on stage, we will use it for the LINAC4 experiment in early 2018. However, in order to assure the operability of such a system for the ESS lifetime a lot more R&D will be needed.

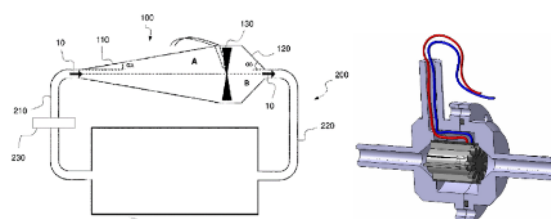
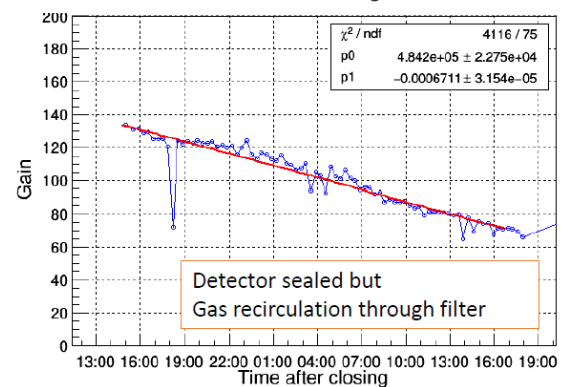
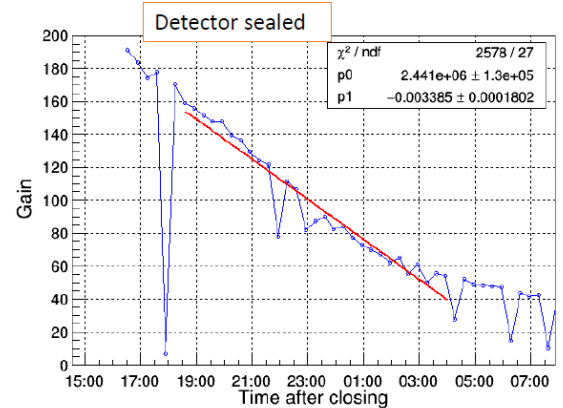
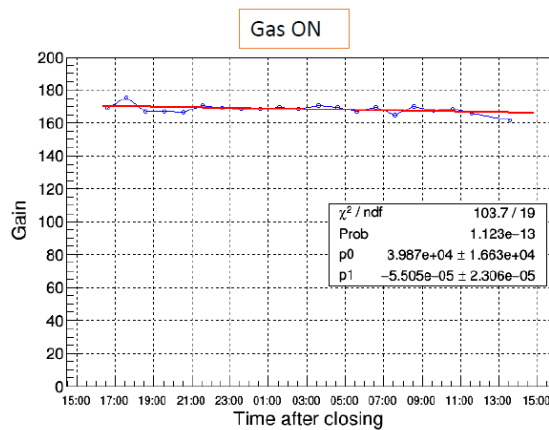


Figure 11: Turbine of the close recirculation system to use during the nBLM tests at LINAC4.

In November, we test the CAPS with the 1st prototype of HARPO (a small turbine and pipes in plastics) with the slow nBLM module. We took data with a Cf-252 source, first when the detector isn't sealed, and we observe that the gain is stable, as shown in Figure 3 a. When the detector is sealed we observe a steady degradation of the gain and after 24h of operation, there is no signal. After we turn the CAPS


on, the gain is decreasing at a different slope and we can operate for longer time as shown in the image below. However, this is no long enough for the tests at Linac4.



Therefore, three more CAPS systems are under fabrication, with a powerful turbine (longer lifetime) and every pipes/ valves/etc/ in metal to reduce the outgassing and the possible leaks. The system will be tested by the beginning of next year hoping to reach a good and stable behaviour for all the LINAC4 experiment.

3.4. Tests planned for 2018

Different tests are foreseen to be done between the end of November 2017 and the delivery of the final CDR, to fully characterize the response of the nBLM detectors and its electronics. In document [3] we already discussed them, however some of the proposed facilities are not operative anymore and we have looked for alternatives to cover the proposed studies. In addition, new opportunities have arrived and are also explained in this document. The different facilities are listed in Table 2 and the new planning is shown in Table 3. In most of the studies we plan to use the new discussed detectors. Note that, due to the unique conditions of operation of the ESS facility, only the commissioning and the studies performed on-site will fully allow to set the operation point of the nBLM system. The test at LINAC4 is the one the closest to the real conditions and the most important. During the test, the full electronics chain will be tested.

	nBLM Project – CDR1.1	CEA-ESS-DIA-RP-0033
	ESS-I	Page 20 sur 43

A new test that has appeared is to install the nBLM detectors at IPHI accelerator (present in CEA/Saclay) for the next planned production of neutrons happening in January or February 2018. Although we will not have an exact value of the initial rate, we could complement the efficiency studies with relative measurements. Moreover, the debug of the electronics can also be carried out during these tests. The advantage of the test is that the facility is at CEA/Saclay simplifying the installation and availability of the tests.

Test Facility	Particle	Energy Max	Test	Date	Comments
Birmingham MC40	Protons to material target	28 MeV	- Study response under different loss scenarios - Electronics ageing	Nov-17 + some date in 2018	Detector can be left there. We can go back in 2018 also with new detector
LINAC-4	Protons	160 MeV	RF backgrounds and response to losses	Feb-April 2018	Installation in January Need to have in place the closed circulation of gas
ORPHEE CEA/Saclay	Thermal neutrons		Response to thermal neutrons		
Amande (CEA/Cadarache)	Mono-energetic neutrons	From 250 keV to 15 MeV	Efficiency studies. Different poly and convertors thickness	Feb or March 2018 (6 days)	Presentation for acceptance the 7th Dec
IPHI	Neutron production	1MeV	Response study for different energies	From January 2018	Different slots can be planned
Upssala	Testing the ESS cryo-modules		Response to RF backgrounds	From January 2018	

Table 2: List of the proposed tests at different irradiation facilities to characterize experimentally the nBLM detectors

	Nov. 2017				Dec. 2017				Jan. 2018				Feb. 2018				March 2018				April 2018			
Test Facility	W1	W2	W3	W4	W1	W2	W3	W4	W1	W2	W3	W4	W1	W2	W3	W4	W1	W2	W3	W4	W1	W2	W3	W4
Birmingham																								
LINAC-4																								
ORPHEE																								
CEA/Cadarache																								
IPHI n																								
Cryo. at Uppsala																								

Table 3: Planning for the listed tests in Table 2 at different irradiation facilities with the nBLM detectors

There are other facilities or tests under consideration. The most relevant one is:

- Looking for a gamma radiation facility. Originally it was proposed to use CoCase but is no longer operative. **Add test Philippe is looking into.** We have identified Pagure in CEA/Saclay that is very expensive. Another option could be tests at Lund proposed by Irena.

Other possible studies are:

- The cryomodules are going to be tested also in CEA/Saclay. However the RF power will not be maximal. In any case it could be used as a partial test and also as a possible test of the final electronics as they will be tested in Saclay.
- The test at Birmingham is proposed for November 2017. We will use the prototypes we have now operational. The detector can be left on-site for further tests and to study the ageing of the amplifiers. In addition, an extra data campaign can be organized with the new designed detectors.
- In Saclay another facility was identified, the *Laboratoire national Henri Becquerel* (LNHB), to perform relative studies of the efficiency of the detector when changing the polyethylene or convertors thicknesses using an intense Cf-252 source. This facility can be a back-up in case the proposition for Amade is not selected or the test at IPHI is delayed.

4. Electronics overview

In this section, a general overview of the electronics is discussed. In Figure 12 the architecture is shown.

The signal produced in the detectors is amplified and then acquired in the BEE. In the next section details of the FEE are discussed in detail. The BEE hardware design is shown in section 6. In Section 7 the control system design is presented. In this section the components of the HV and LV are presented in detail.

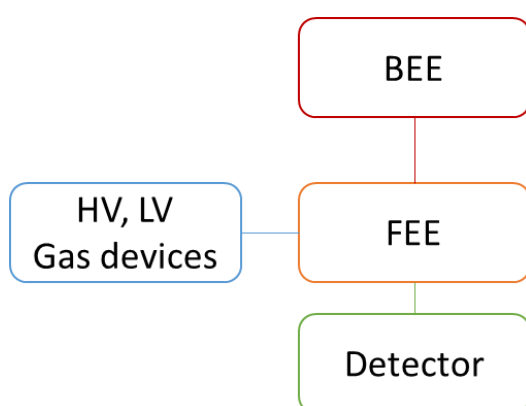




Figure 12: Overview of the electronics architecture. From the signal produced on the detector and amplified in the FEE to the BEE. The detectors need voltages for the detector and for the FEE.

4.1. Electronics components

- FEE: described in section 5
- High Voltage and Low Voltage modules: described here
- BEE and acquisition cards: described in section 6
- System controls: described in section 7

 	nBLM Project – CDR1.1	CEA-ESS-DIA-RP-0033
	ESS-I	Page 23 sur 43

4.2. Hardware for High Voltage and Low voltage

The detector needs two HV inputs, one for the mesh and one for the cathode (or drift). In addition, it needs the power of the preamplifiers that are placed on-board of the detector, i.e in the accelerator tunnel. For the choice of the modules the compatibility with EPICs needs to be taken into account for the controls of the system as required by ESS-ICS.

Therefore, the CAEN SY4527 crate system has been chosen to power the HV and LV modules. The EPICS IOC is integrated in the CPU of the crate. The HV and LV cards chosen will be integrated in the module.

4.2.1. Crate CAEN SY4527

To power the HV and LV cards the crate CAEN SY4527 has been chosen. This crate is EPICs compliant. Images are shown in Figure 13. More information about its characteristics can be found in [CAEN SY4527](#). The dimensions of the mainframe are 19"-wide, 8U-high euro-mechanics and it hosts four main sections:

- The Board Section, with 16 or 10 slots to house boards, distributors and branch controllers
- The Fan Tray Section, housing 6 fans arranged on two rows, with programmable rotation speed regulation;
- The Power Supply Section, which consists of the primary power supply and up to 3 power supply units. In principle with one for our system can be enough although an extra one is foreseen to increase the reliability of the system.
- The CPU and Front Panel Section which includes all interface facilities.

The CPU controller is available in 3 different versions, we have chosen the BASIC option that fulfil all our requirements. It provides all the communication interfaces, the RESET control, the INTERLOCK control and status LEDs.

The extra power module we propose to include is the [A4532](#) Optional Single Power Supply Unit 600W. It fits in one slot.

With the fix distribution of detectors, two SY crates will be installed at the low and high energy regions of the accelerator.


	nBLM Project – CDR1.1	CEA-ESS-DIA-RP-0033
	ESS-I	Page 24 sur 43



Figure 13: Front panel with the LCD screen controller and back front with 16 HV cards in place and the power input of the SY4527 crate. Images taken from CAEN webpage. The crate will be use to power the HV and LV cards of the nBLM system.

4.2.2. High Voltages

The card CAEN [A7030](#) have been chosen for the HV of the Mesh and Drift of each Micromegas detector. The cards can house 12, 24, 36 or 48 independently controllable High Voltage channels. Common floating return is shared by all channels. It can goes up to 3kV. The MMs voltages will not exceed 1.5kV. The monitoring resolutions are 5mV voltage and 2nA current, important parameter to assure the correct operation of the MMS detector.

Depending on the number of channels the connector in the card is SHV or radiall 52 pin connector. For 84 detectors each one needing 2 HV inputs, 168 channels are required covered with 4x48 channels cards. The adaptor [R648](#) will be used to go from the pin connector to SHV connector. This module has to be placed in the rack, its size is one unit in a 19" wide rack. A figure of the card and the adaptor are shown in Figure 14. It is in fact as a patch panel. From the rack the cables will be driven to the accelerator tunnel through the stubs to the patch panel in the tunnel.


	nBLM Project – CDR1.1	CEA-ESS-DIA-RP-0033
	ESS-I	Page 25 sur 43



Figure 14: HV card CAEN A7030 with the adaptor R648 from radiall 52 pin to SHV connectors for the HV of the nBLM detectors. Images taken from CAEN webpage.


The SY4527 crate with one 48 channels A7030 card and the R648 adaptor have been received and tested with one nBLM slow detector showing performance as expected. It was left in operation during a week and no problems were found.

4.2.3. Low voltage

For the LV the card [A2519](#) has been chosen. It has eight individual floating controllable low voltage channels. The requirement for the preamplifiers is to provide $\pm 5V$ and a GND connection. The module has also independent ground per channel. The output voltage range is $5 \div 15 V$, (1 mV steps) with 1 mV monitor resolution and the maximum output current is 5 A (10 mA steps) with 1 mA monitor resolution. The RAMP-UP and RAMP-DOWN Times may be selected independently for each channel in the $1 \div 200 ms$ (1 ms step).



Figure 15: LV module CAEN A2519 for the power of the nBLM preamplifiers. Images taken from CAEN webpage.

	nBLM Project – CDR1.1	CEA-ESS-DIA-RP-0033
	ESS-I	Page 26 sur 43

5. Front-End Electronics

For the nBLM detectors the front-end electronics (FEE) is placed on-board of the detector in the accelerator tunnel. The signal is amplified by fast amplifiers before sending it to the back-end electronics placed at a maximum distance of about 80 meters through a low loss transmission cable.

The idea is to have mezzanine cards for the reading of the signal and for the detector HV power. A general view of the design is shown in Figure 16. Therefore, the PCB where the Micromegas is routed has also connectors to connect to these cards. These mezzanine cards are explained in the first subsection of this section (5.1). The design of the Micromegas card was presented in section 3. In addition, in this section we describe also the cables and the connectors proposed.

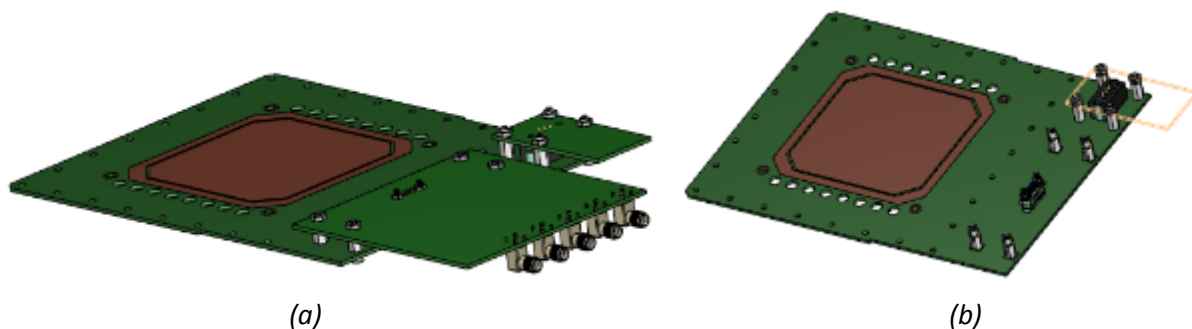


Figure 16: (a) Assembly of the three PCB boards: mother board with the MMs detector. On the left the signal mezzanine card and on the right for the HV. (b) Mother board with the MMs explained in sub-section 5.1, the connectors to the other boards are also shown.

5.1. PCB designs

5.1.1. Signal read mezzanine card

The detector is segmented in 4 strips to adapt for high neutron fluxes if needed in the high energy region of the accelerator. However, only one output signal per detector is read and send to the BEE. This output signal will be the sum of the four strips or of just 1, 2 or 3 channels. In Figure 17 the design is shown. Jumpers will allow us to decide if we read 1 or the 4 channels. Once set, the combination of the channels to read is send to the preamplifier.

The front-end module have been designed by Philippe Legou. They are fast amplifiers called *FAMMAS* (Fast Amplifier Module for Micromegas ApplicationS) [5]. The modules can be adapted in Gain and Noise filtering (decide bandwidth). The preamplifier has a quiescent current of 10mA, which means a consumption of 100 mW. We propose to have two possible outputs paths in case one fails for any reason. In any case a manual intervention in the tunnel will be required to change from one output

to the other. After the preamplifier an output driver buffer is placed to assure the transmission over the long cable. The quiescent current for one buffer is 15mA, so for one buffer the consumption is 120mW. The polarization voltage for the preamplifiers is +5V and -5.2V.

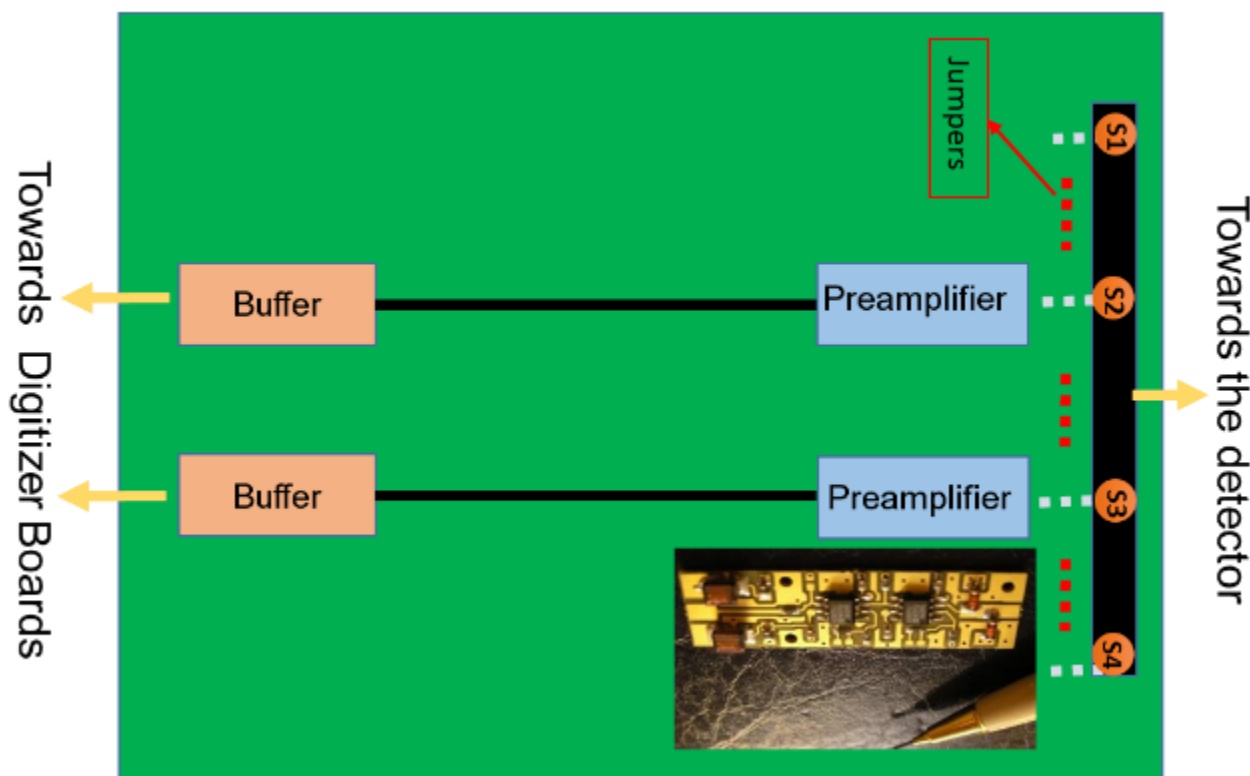


Figure 17: nBLM FEE card to read the signals from the detector.

The card has dimensions of 100x100mm. It also includes the power of the preamplifiers.

The connector we propose is a Harwin Gecko Screw-Lok Vertical DIL PC Tail Connector, with reference G125-MV11005M2P and G125-FV11005F1P (male and female respectively), shown in Figure 18. They are Halogen-free, PFOS-free, SVHC-free and RoHS compliant. Their composition is Glass-filled High Temperature Thermoplastic UL94V-0 for the base and Beryllium Copper Phosphor Bronze for the connectors. The screws and latches are made by stainless steel and copper alloy. Some quantity of gold and nickel is also present. In principle these materials are radiation resistant for the ESS levels quoted in [6]. For the polyamide, values are found in [7]. In any case, experimental studies can be carried out at Birmingham MC40 irradiation facility.



Figure 18: signal connectors proposed for the nBLM detectors. Image from Harwin.

5.1.2. HV mezzanine card



This card will be composed by a HV connector that will be connected to the HV cables coming from the HV card in the gallery and by a filter.

The connector we propose is a Harwin M300 SIL Vertical PC Tail Connector. The exact reference is M300-FV1034500 and M300-MV10345M1 (female and male). It has 3 pins, two for the HV (mesh and drift) and one for the ground. An image from their website is shown in Figure 19. They are RoHS Compliant - 2011/65/EU, and as quoted in his information they do not contain lead, brominated flame retardants red phosphor or antimony. In addition they are used in the aerospace equipment. The composition is Glass Filled Thermoplastic UL94V-0, the female contacts are made by Beryllium Copper, the Male contacts by Brass. And there is also gold and stainless steel present. They are therefore also radiation resistant for ESS values.



Figure 19: HV connectors proposed for the nBLM detectors. Image from Harwin.

In addition, there will be a HV filter, made by an R-C-R circuit to suppress the noise from the HV source.

 	nBLM Project – CDR1.1	CEA-ESS-DIA-RP-0033
	ESS-I	Page 29 sur 43


5.2. Cables and patch panels connectors

NEEDS TO BE COMPLETED

There will be cables from the rack down to a patch panel in the tunnel and from the patch panel to the detectors. They should have the same impedance and characteristics. The connectors in the patch panel are also very important in order to match the impedances.

For the cables we have chosen *TO BE COMPLETED*

Cable type		ESS data base number
HV cables		
Signal		
LV	± 5V	
	GND	

	nBLM Project – CDR1.1	CEA-ESS-DIA-RP-0033
	ESS-I	Page 30 sur 43

6. BEE and Acquisition

In this section the hardware of the BEE is discussed. Details are given in document “*nblm_control_system_design.pdf*” send together with the documentation of the CDR1.1.

For the fast acquisitions (BEE), the architecture is ICS compliant. We use a MTCA crate with a power module, a MCH board and one or several AMC board recommended by ICS: the IOxOS IFC1410 board. The IFC1410 board has 2 FMC port where we will connect one or two ADC-3111 acquisition board also compliant with the ICS recommendation.

6.1. MTCA crate



The IOxOS IFC1410 board is connected to a MTCA crate. It is composed by a cooling unit, a power module, a backplane and a MCH board are the basic minimum configuration. The communications between AMC and MCH are done through the backplane.

- MCMC : MicroTCA Carrier Management Controller
- MCH : MTCA Carrier HUB
- MMC : Module Management Controller
- AdvancedMC : AMC : Advanced Mezzanine Card
- EMMC : Enhanced Module Management Controller
- PM : Power Module
- CU : Cooling Unit
- μ RTM : MicroTCA.4 Rear Transition Module

6.2. Fast acquisition

ICS standardisation for fast acquisition is based on MTCA.4, the IOxOS CPU IFC_1410 and IOxOS ADC_3111 FMC boards. IOxOS Technologies provides the IFC_1410, a MTCA.4 Intelligent FMC Carrier in AMC form factor featuring NXP PPC QorIQ processors of T Series and Kintex UltraScale FPGA devices. The IFC_1410 can carry 2 FMC boards ADC_3111. The input voltage range is -0.5V to +0.5V. Each FMC ADC-3111 can read up to 8 analogue signals.

As the timing response of the detector is very fast (at the level of ns) and the total duration of an event is of the order of 100-200 ns, the acquisition speed of 250 Msps of the FMC board is enough.

 	nBLM Project – CDR1.1	CEA-ESS-DIA-RP-0033
	ESS-I	Page 31 sur 43


6.3. FPGA software

The FPGA software development will take in charge the requirements presented in the document *“Requirements and functions to be implemented for the nBLM control system”* [8].

The FPGA will have 3 main tasks:

- Detection of neutrons and counting
- Trig an alarm on the Beam Interlock System if needed
- Supply of debug and diagnostic data (neutron rates ...)

The FPGA software design and development will be done by ESS ERIC. ESS-I will support this task with the procurement of the analysis algorithm. In document [9] the FPGA firmware specifications are described in more detail. Note that it is not yet a final document.

	nBLM Project – CDR1.1	CEA-ESS-DIA-RP-0033
	ESS-I	Page 32 sur 43

7. nBLM Control system

The control system overview architecture is presented in detail the document that accompanies this CDR1.1 “*nBLM Control System.pdf*”. In the document the analysis algorithm to be introduced in the FPGA is also discussed. Moreover, the development of the GUI for the low Control System is also shown.

8. Gas system status

Regarding the gas system there have been small modifications with respect what the design proposed in PDR12, where more details about the system can be found. The proposed changes are summarized in the following:

- Install 20 lines into the tunnel (10 distribution lines + 10 return lines). With the new detector’s distribution discussed in section 11, it is more reasonable to have two extra gas lines for the ones placed at very long distance from the source.
- Increase patch-panel number to 6 (more details about position of them in Section11).
- Include two pumping points to have the option to pump the whole system from outside the tunnel (see Figure 20).
- By-pass all the controllers with manual ones to increase reliability to the system
- Include bubbler at the end of the exhaust line to increase reliability to the system
- Enclosed the manometer in the gas bottle storage cabinet with key.

The gas system consists in 4 parts:

1. The bottle storage area outside the building
2. The gas rack where we have the control command
3. The distribution and return lines from (to) the rack to (from) the accelerator tunnel
4. The detectors localization where the lines will connect to each module

The design of the system going from the bottles to the controller rack and from the rack to the accelerator tunnel has been finalized in order to fit to the ESS installation schedule. Extra resource was needed (Fredrik Persson) due to the very tight time constraints to include the design into the EPL.

As indicated in the list of proposed changes, the distribution system will consist in 10 in lines and 10 return lines to feed 10 groups of detectors. The pipes are made in stainless steel with dimension 6/8 mm (inner/outer). At the end of each one they will be connected to patch panels. Until the installation of patch panels is done they should be close with a cap. All the connectors are Swagelok connectors.

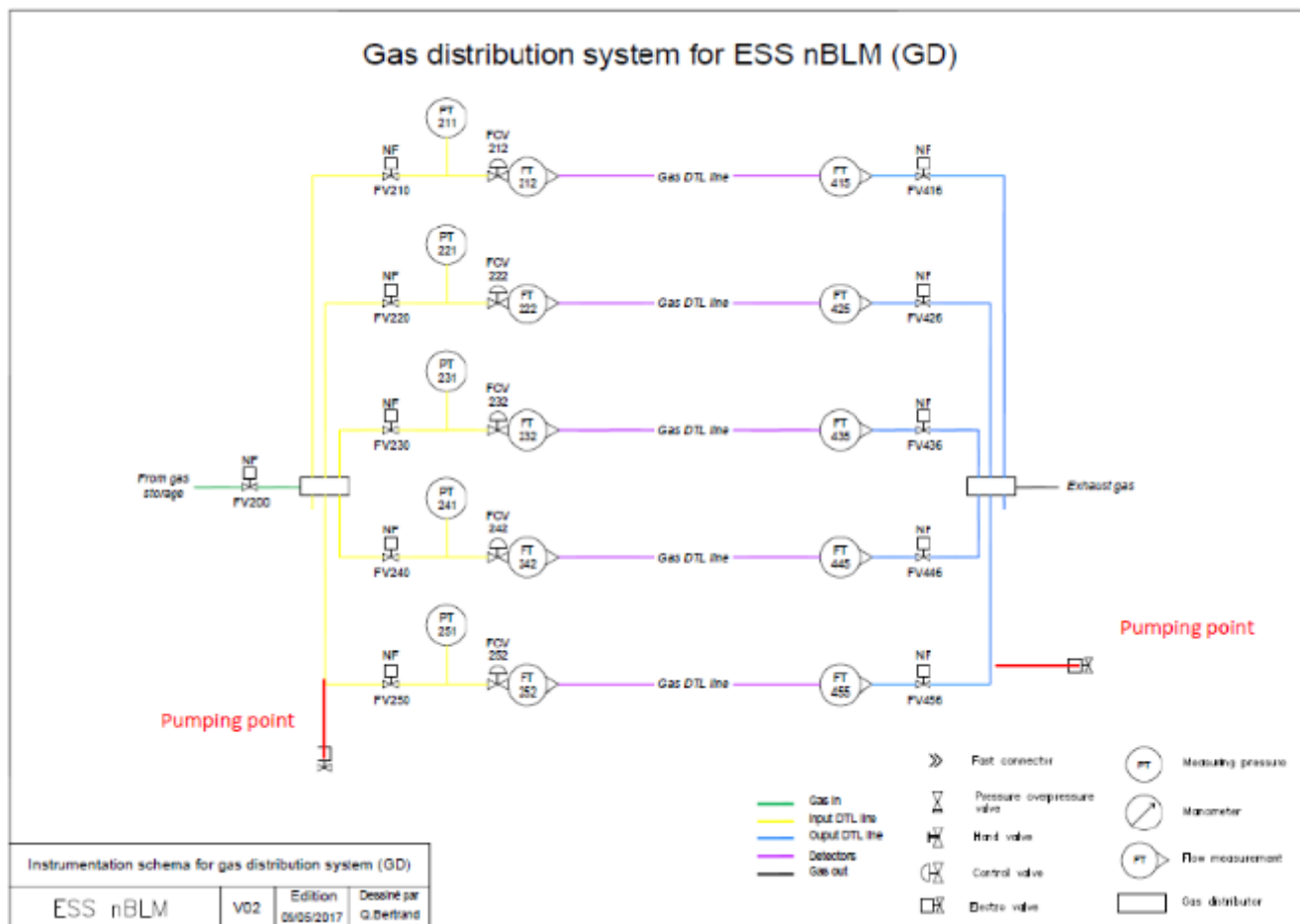



Figure 20: Gas distribution system for nBLM system. The distribution and return lines are sketched. We propose to install 10 of each (and not 5 as sketched) one for each the detector group. Flowmeters at the entrance and exit of each line permit the control of leaks in each group of detectors and the electrovalves allow the isolation of one line without affecting the rest of the system in case of an intervention in one detector.

9. nBLM systems risk analysis

From the review of the PDR1.2 an analysis of possible system failures regarding the amplifiers, the gas, etc was requested. We have prepared an independent document send together in this CDR1.1 documentation package that tries to cover the possible risks in each subsystem of the nBLM system (gas, FEE, BEE and detectors) giving a mitigation strategy as well. Some of them will implied an increase in the initial allocated budget and will need to be reviewed and further discussed together with ESS. The referred document is *nBLM_subsystemsRiskAnalysis.pdf*.

	nBLM Project – CDR1.1	CEA-ESS-DIA-RP-0033
	ESS-I	Page 34 sur 43

10. nBLM system architecture at ESS

In this section the plans for the integration and installation of the system into ESS is discussed. The distribution of the detectors along the linac is presented. This distribution has been fixed now and therefore there are some differences with respect what was presented in [4]. In addition, the distribution of the electronics in the different racks, the gas lines distribution and the patch panel position are discussed. The distribution of the acquisition cards in racks and of the cables through the stubs have been carried out by the BI-ESS, in discussions with CEA, trying to optimize cable length and the required system redundancy. Furthermore, an initial design of the detectors support is shown.

10.1. Distribution of nBLM detectors along the accelerator

The distribution of the positions of the 84 detectors have been decided. The support of the detectors will be designed flexible to have the possibility to move the detectors during the commissioning of the machine to find the most optimum position for the detection of losses around this position. Moreover, this allows also to move them during the beam tuning to interest hot points.

Most of the detectors will be placed in the DTLs and Spokes. Each DTL will be covered by 4 slow and 4 fast detectors. An extra pair of fast+slow will be placed at the end of DTL-5. Each spoke will have one fast and one slow detector. The fast will be placed in the quad and the slow in the cryomodule. Four will be also placed in hot spots of the MEBT in two different positions. The rest will be put in the cold linac: one pair of fast+slow in the Medium Beta and another in the High beta. Three more pairs of fast+slow will be placed in the target area. The distribution is shown in Figure 21 and listed in Table 4. Notice that with this distribution we have 82 detectors installed of the 84 to be delivered, i.e. there are one spare of each one. In addition with the installation of detectors up to the target region we will have to install ~500m pipes for the gas.

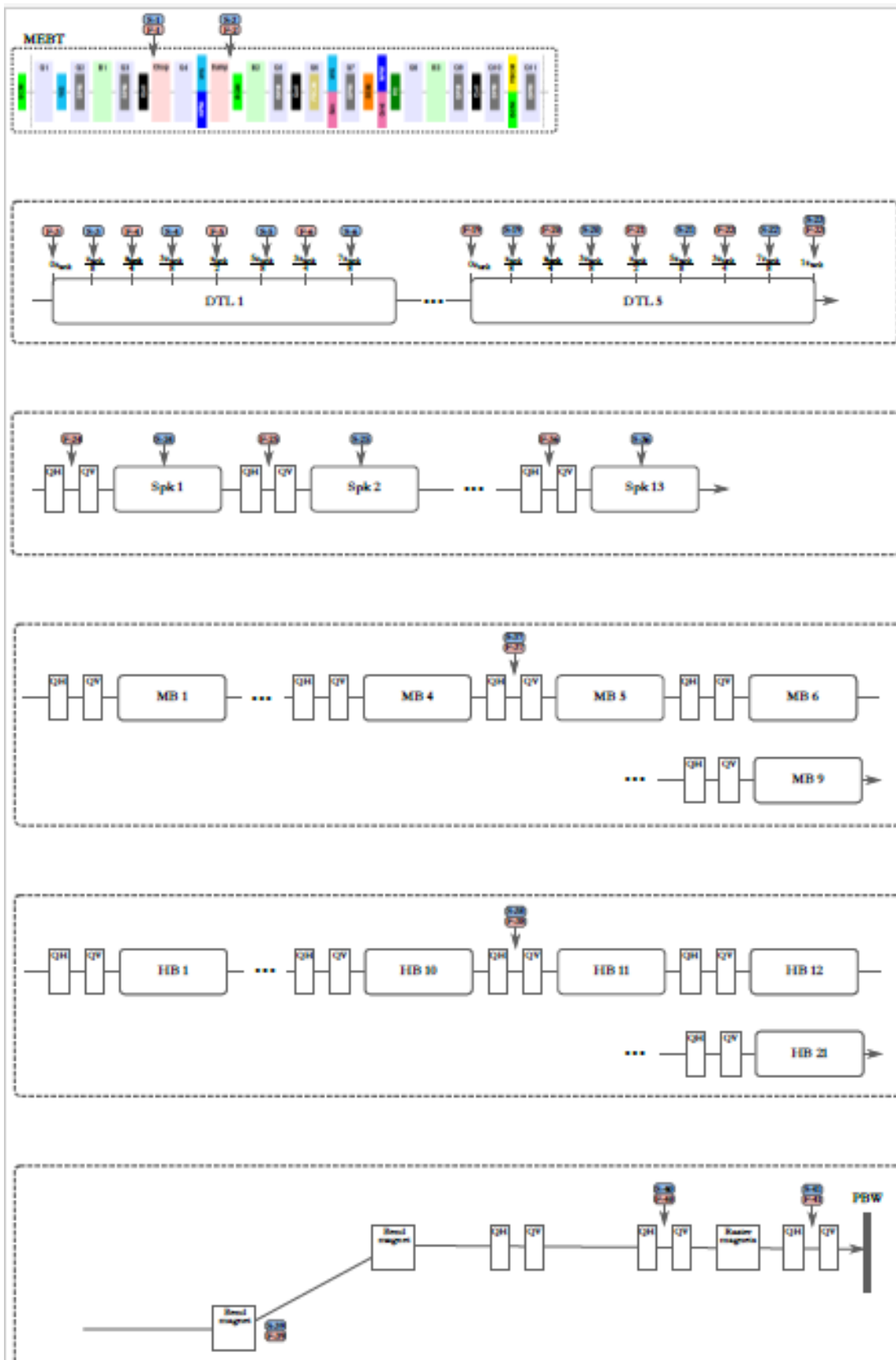


Figure 21: Distribution of the nBLM modules along the accelerator.

	TOTAL NUMBER OF DETECTORS	DETAILED DISTRIBUTION
MEBT	4	2xFast + 2xSlow
DTL	42	(4xFast + 4xSlow)/DTL
SPK	26	(1xFast + 1xSlow)/SPK
MB	2	1xFast + 1xSlow
HB	2	1xFast + 1xSlow
PBW	6	3xFast + 3xSlow
TOTAL	82	

Table 4: listed of nBLM detectors along the different accelerators sections

10.2. Detector acquisitions and racks distribution

The distribution of the detectors to the FMC cards has been also done. Each ADC311 FMC has 8 channels and each IFC1410 board can integrate two FMC cards. However, only one FMC card per IFC will be install having an extra slot free in the IFC.

Moreover, to avoid blind sections in case of a hardware failure (IFC1410 or ADC311), it has been decided to cross detector pair on different ADC311 modules.

The distribution of the MTCA crates per rack is shown in Table 5. Note that more than a MTCA is connected to the same rack in some cases. This proposed distribution, however, implies the use of 18 FMC that will overhead the allocated budget in a 63% (or 28k€) due to the price per channel of 500€.

Rack	#detectors connected	#detectors per FMC "(), " marks new crate	#FMC (=#AMC)	#crates	Spare signal cables per rack
FEB-050ROW	22	(6+5), (6+5)	4	2	2
SPK-010ROW	22	(6+5), (6+5)	4	2	2
SPK-030ROW	14	(5+5+4)	3	1	2
SPK-050ROW	14	(5+5+4)	3	1	2
MBL-050ROW	2	(2)	1	1	4
HBL-090ROW	2	(2)	1	1	4
HEBT-030ROW	2	(2)	1	1	1
A2T-010ROW	4	(2)	1	1	1
Sum	82		18		18

Table 5: rack distribution of the ADC311 FMC cards (i.e. of the MTCA crates).

10.3. Power supplies distribution

For the power supply of the system the hardware components are discussed in Section 4.

- For the HV two cables are bring individually to each detectors (mesh and drift).
- For the LV 3 inputs are needed per detector (+5V, -5V and GND). However, we can group the detectors and install only one set of 3 cables per group or use a triple cable. Once in the tunnel, they will be connected to the patch panel and then distributed to each detector per group. We will group the detectors in 10 groups as for the gas lines (see section 10.4).

In order to cover the full accelerator it is better to install two SY crates instead of one to reduce the length of the HV and LV cables for the detectors placed at the high energy region of the accelerator. The distribution of the power cards per SY crate and per rack is shown in Table 6.

Rack	#detectors connected	Location of the connected detectors	#HV cards	#LV cards
FEB-050ROW	76	all det. up to including HBT	4	1
A2T-010ROW	6	all det. in A2T and HEBT	1	1

Table 6: Distribution of SY4527 crates and HV and LV cards

10.4. Gas lines distribution in the accelerator

For the gas system, 10 distribution + 10 return lines will be installed into the accelerator tunnel that will bring the gas and return it back for 10 groups of detectors. Originally we propose 8 groups, however, with the new distribution of detectors up to the PBW region, we consider more reliable to install two more to feed the detectors up to this regions.

The gas lines will go from room FEB-090, where the gas rack will be installed, to G01 through that shielding wall. Once in the tunnel they will be connected to patch panels placed at different locations and from there distributed to the corresponding group of detectors. We propose to install 6 patch panel with the same design to allocate up to two gas lines, although in some of them we will only connect 1. In Table 7 the position of the gas patch panel, the lines of gas connected to it and the group of detectors connected per gas line are shown.

The group of detectors have been defined taking into account the proximity between the detectors and to have a maximum number of detectors per line. In this configuration, we will not have spare gas lines however, the maximum number of detectors per line has not been reached in most of them giving the possibility to connect a 50% more detectors (i.e. up to 12) per line. A sketch of the distribution is shown in Figure 22 in general and in Figure 23 in detail for one group of detectors.

Detectors in	Gas line	Patch Panel (PP) Number	Position of PP (aprox.)	Number of detectors
MEBT-DTL1	Line 1	PP-1	end DTL1	12
DTL2	Line2			8
DTL3	Line 3	PP-2	end DTL3	8
DTL4	Line4			8
DTL5	Line 5	PP-3	end DTL5	10
SPK1-4	Line6			8
SPK5-8	Line 7	PP-4	end SPK8	8
SPK9-13	Line8			10
MB-HB	Line 9	PP-5	beginning of HB region	4
	No line			No line
Bend Magnet	Line 10	PP-5	somewhere after magnet	6
	No line			No line
Total lines	10			

Table 7: Distribution of detectors per gas line and number of patch panels.

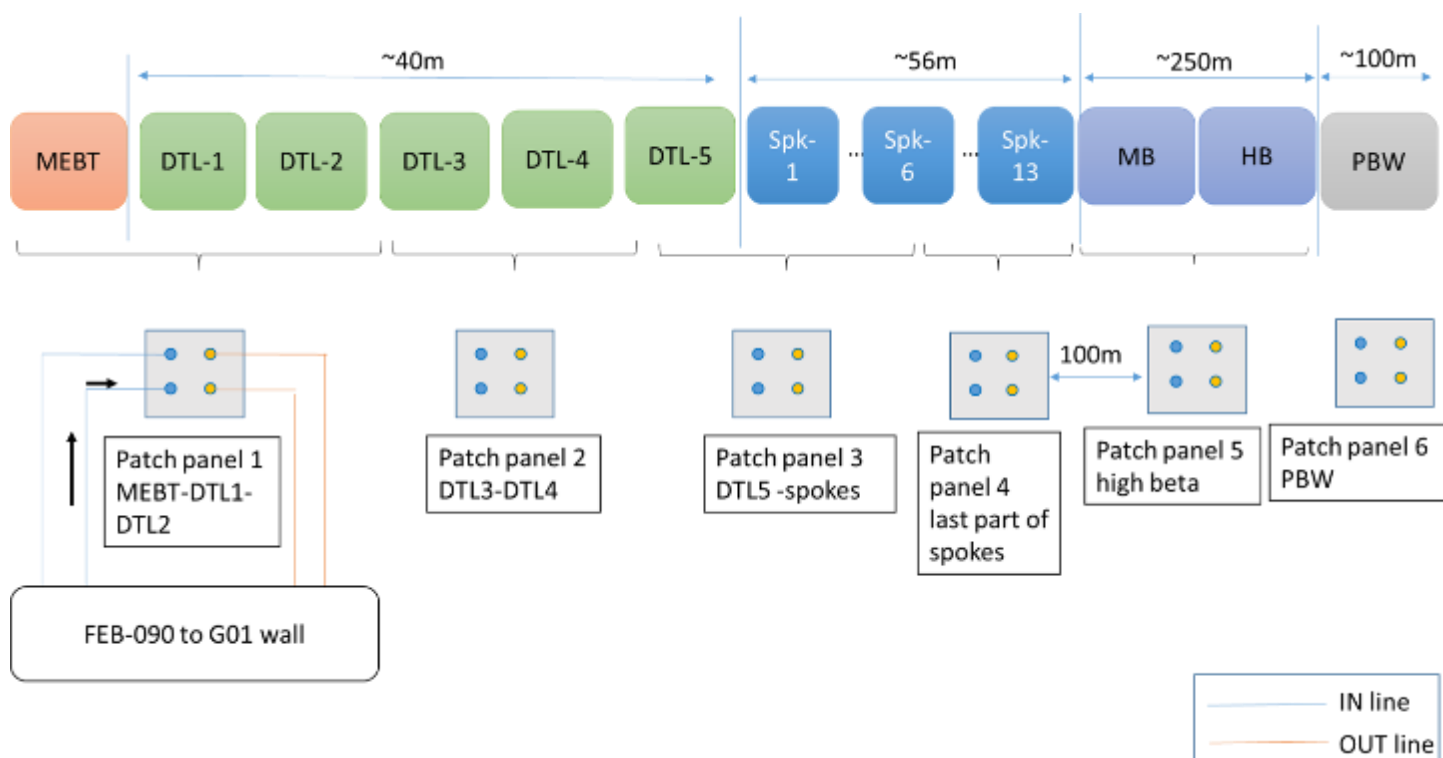


Figure 22: Sketch of the position of the gas patch panel.

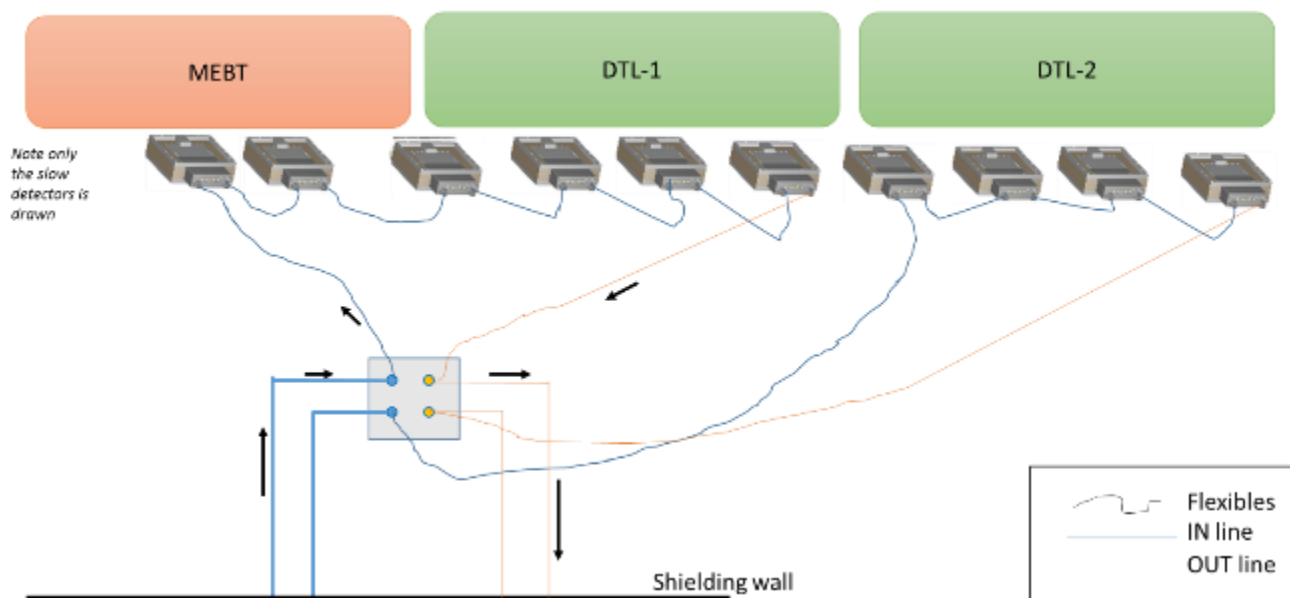



Figure 23: Detail of one nBLM gas distribution patch-panel. Note that only the slow modules have been drawn for simplicity.

With this gas line distribution we have also calculated for how long we have to recirculate the gas in order to reach the require gas purity for stable gain operation after installation or after an operation that implies the enter of air in the system. We have assumed that the detectors will be installed filled with gas and closed. In addition, we assume the rest of the system is pump down. With these

	nBLM Project – CDR1.1	CEA-ESS-DIA-RP-0033
	ESS-I	Page 40 sur 43

assumptions for most of the lines the time required is of ~4hours, except for the one in the HB section (8h) and the one in the PBW section (17h). This have been calculating assuming we need to change five times the gas volume. However, if air enters in all the detectors in a line we have to multiply this number by four (renew 20 times the volume).

10.5. Position and preliminary design of patch panels in accelerator tunnel

The position of the patch panels has been discussed in previous section. We propose to install 6 gas patch panels and 12 (or 6 double) patch panels for the cables connectors. The approximate position of the patch panel are listed in Table 7.

10.5.1. Gas in accelerator tunnel

Each patch panel will receive two input lines from the gas rack and two return lines from two group of detectors. As discussed previously there are no spare gas lines foreseen although more connectors can be connected to the existing ones. Therefore, we propose a by-pass system of valves in the patch panel to have the possibility to pass one set of detectors to the other gas line in case of big leak in one distribution or return line. An sketch is shown in

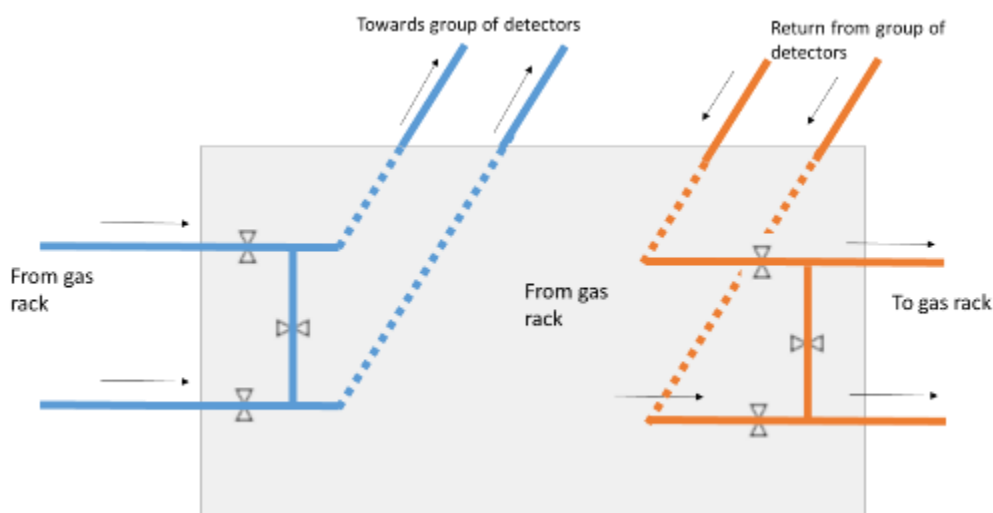



Figure 24: We will predict the best connectivity logic in order to have the possibility to interconnect the two sets of detectors at one line in case a leak is observed in the other.

	nBLM Project – CDR1.1	CEA-ESS-DIA-RP-0033
	ESS-I	Page 41 sur 43

10.5.2. Electronics patch panel in accelerator tunnel

One cables patch panel is foreseen per group of detector. The maximum number of detectors per group is 12. Assuming an extra 25% spare connector, mean connectors for 15 detector. Therefore we propose patch panels with:


- 60 HV connector (30 HV IN, 30 HV OUT)
- 48 LV connectors (3 IN, 45 OUT)
- 30 signal connectors (15 IN, 15 OUT)

10.6. Preliminary design of detectors support structure

In this subsection some initial ideas about the detectors support structure are shown. We propose to design a rail along the different sections. For example, we could install one per DTL and Spoke. It can be attached to the floor or to the accelerator. For the sections where only one or two set of detectors are foreseen, as in the MEBT, MB, HB and PWB, an individual support can be more adequate. However in this case the most ideal will be to attach it to the floor. In that sense discussion have started to coordinate the integration of it in the 3D model. Initially we propose to place it a vertical plane parallel to the accelerator axis. The height with respect the floor has to be decided.

A preliminary proposition is shown in Figure 25. The support in this case is for attachment vertically although a horizontal one can be similar. Each detector can be attached independently into the rail and be move easy along it manually. In addition, both detectors can be attached together.

Some simulations studies are on-going to study if the response changes, for the fast detector, if we placed it with a given angle with respect the beam instead of facing it (parallel to x-y plane). The design can be done in order to accommodate the detectors with a given angle. Along the rail we propose to have an extra kind of cable tray or cables tights where to place the cables and gas tubes that connect to each detector.

	nBLM Project – CDR1.1	CEA-ESS-DIA-RP-0033
	ESS-I	Page 42 sur 43

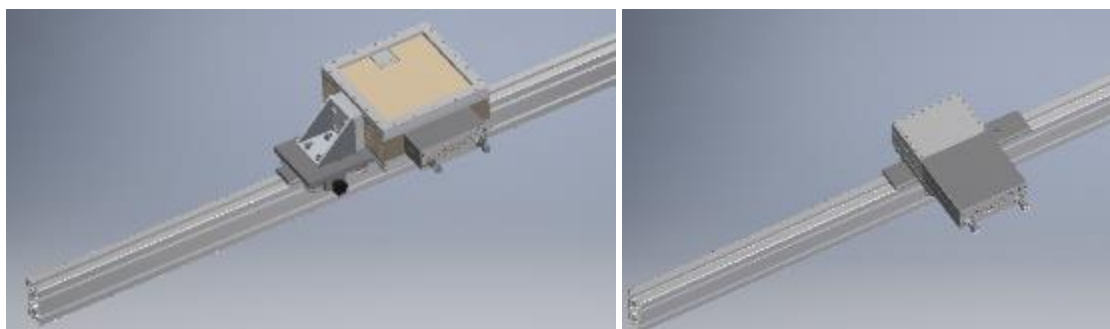




Figure 25: (Top) Conceptual design of the possible support structure for the nBLM detectors. (Medium) Closed view of the support of the slow and fast detector, respectively.

10.7. Procurement of components

To be discussed during CDR1.1 presentations and updated later in documentation.

 	nBLM Project – CDR1.1	CEA-ESS-DIA-RP-0033
	ESS-I	Page 43 sur 43

11. References

- [1] ESS, “nBLM and icBLM PDR,” ESS-0123083, 2016.
- [2] Y. Giomataris Ph. Rebourgeard J.P. Robert G. Charpak, “MICROMEGAS: a high-granularity position-sensitive gaseous detector for high particle-flux environments,” *NIM A*, vol. 376, no. 1, pp. 29-35, 1996.
- [3] L. Segui et al, “PDR1.1,” CEA-ESS-DIA-RP-0013, (ESS-0110762), 2016.
- [4] L. Segui et al, “nBLM PDR1.2,” CEA-ESS-DIA-RP-0027, 2017.
- [5] P. Legou, “A New High Rate Charged Particles Detector,” *39th ICFA Advanced Beam Dynamics Workshop*, p. <http://accelconf.web.cern.ch/AccelConf/abdw06/PAPERS/WEBZ03.PDF>, 2006.
- [6] ESS, “Material classification to radiation resistance in the ESS linac tunnel,” ESS-0007659.
- [7] CERN, “CERN-HS-RP-093”.
- [8] L. Segui, “Requirements and function for the nBLM control system,” CEA-ESS-DIA-RP-0024, 2017.
- [9] Y. Mariette, “nBLM Control System,” 2017.
- [10] S. Aune, L. Segui and T. Papaevangelou, “Gas Pipes nBLM system,” CEA-ESS-DIA-NT-0020, 2017.